AADE-06-DF-HO-05

A Comprehensive Bit Hydraulics Model for Gasified Drilling Fluids

Dogan, Huseyin Ali, Turkish Petroleum Co., Ankara-Turkey
Gucuyener, Ismail Hakki, Turkish Petroleum Co., Ankara-Turkey
Ozbayoglu, Evren, Middle East Technical University, Petroleum & Natural Gas Eng. Dept., Ankara-Turkey

Abstract

This study presents a mathematical model for calculating bit pressure drop for gasified drilling fluids. In the literature, there are several studies on determination of the pressure losses for multiphase fluids. The models, however, are either valid for high gas flow rates or developed using very strong assumptions.

The theory, which is valid for both sonic (critical) and subsonic (sub-critical) regimes, is based on the solution of the general energy equation for compressible fluid flow. Unlike the existing models, the proposed model takes change in the kinetic energy, compressibility factor, and internal energy terms into consideration. Moreover, the model uses “a mixture sound velocity” approach for determination of the sonic boundary of the fluid.

By developing a program, the pressure drop through a nozzle could be calculated in the subsonic flow region. The program has been run with reasonable field data. The results have been compared with the results of existing models and less than a 9% variation was estimated.

Introduction

Low pressure drilling, when used while encountering highly fractured low pressure formations and depleted reservoirs, has several distinct advantages over conventional drilling. It eliminates problems such as partial or total loss of circulation, formation damage, differential sticking, etc. In addition, it has been proven that low weighted drilling fluids increase the penetration rate and extend bit life.

It should also be noted that, the effectiveness of bit could also be improved by increasing the hydraulic power that is delivered by the bit. This increase in hydraulic power depends on the pressure drop across the bit.

There have been many attempts to define gasified drilling fluid hydraulics. Like the proposed model in this study, almost the entire mathematical models presented in the literature are based on the general energy equation. Indeed, in the literature, developed mathematical models exist for estimating pressure drop at the drilling bit, but those are all simple forms of general energy equation.

Literature Review

Two-phase flow through a restriction may be either sonic (critical) or subsonic (sub-critical). Most of the models were developed for wellhead chokes and take sonic flow into consideration.

A group of those models are comprised of empirical relationships (Omana[1], Ros[2], Pilehvari[3], Osman and Dokla[4]). These empirical models generally are valid over a range where experimental data were available, but they give poor results when extrapolated out of range.

The other models are theoretical relationships that have been derived from the basic fluid flow principles. Tangren, et. al.[5] derived expressions for velocity of sound and for two-phase flow and sonic flow through a choke. Equation of motion, which was based on the basic laws of continuity, momentum and energy for a mixture, but, the gas phase was assumed to be ideal gas.

Ashford[6] and Fierce[7] used a similar approach to predict the sonic limit pressure. However, the model has an uncertainty and deficiency, which are that downstream pressure cannot be easily determined and that the model fails in subsonic flow.

Sachdeva, et. al.[8] extended the analysis of Ashford and Fierce[7] and proposed an equation to predict the sonic pressure ratio through a choke. It was assumed that the gas phase at the entrance of the restriction is contracted isentropically, but at the downstream of the restriction, the gaseous fraction of the fluid expands polytropically. Therefore, their equations of pressure drop need only one input pressure (upstream or downstream).

Fortunati[9] used a new approach, and developed correlations for sound velocity, sonic and subsonic flow. The developed sound velocity equation however cannot yet be applied for a low gas/liquid ratio. Gould[10] pointed out that for mass fraction of gas less than 0.4 it is not applicable for Fortunati’s work.

Perkins[11] reviewed the thermodynamic basis, and developed a theoretical framework, which is valid for

both subsonic and sonic flow through a choke. The framework was constructed based on the general energy equation. Sonic flow boundary could also be calculated in addition to the sonic flow rate. The Perkins'[11] model can determine variables at any point in the flowing system based on a constant gas compressibility factor and constant internal energy assumptions.

Guo, Harelend and Rajtar[12] used a thermodynamics based approach, and explained the pressure drop equations for the whole drill string and the bit. However, according to Lyons, Guo and Seidel[13], the application of this model is limited when high gas volume fractions are present.

Gucuyener[14], Liu and Medley[15] obtained an implicit equation for the pressure drop through the bit nozzles. The equation is applicable for gal/liquid mixtures. The equation was based on the general energy equation. In their studies, the upstream velocity of the fluid was assumed to be zero. Actually, the velocity difference between upstream and at the nozzle was significantly large. Based on that fact, the assumption is only logical for low gas flow rates or small nozzle sizes. In addition to this assumption, their equation ignores the internal energy term in the general energy equation.

Theory

A bit nozzle can be treated as a restriction in a pipe "space". Both sonic and subsonic flow in may exist the restriction. During sonic flow, the flow rate through the restriction reaches a maximum value with respect to the prevailing upstream conditions. The velocity of the fluids flowing through the restriction is described as sonic (pressure wave propagation) velocity (Gould[10]) and its value depends on the fluid properties. In the case of sonic flow, large turbulent energy losses are ultimately possible because of shock front (Lyons, Guo and Seidel[13]). This shock front is the same as the sonic wall.

According to Perkins[11], the general energy equation is valid for both sonic and subsonic flow. For subsonic flow, the equation shows that a polytropic flow and reversible adiabatic flow occur as the fluid accelerates downstream of the restriction. Sachdeva et. al.[8] stated that during gas flow at the throat, a temperature gradient develops between the phases, resulting in fast heat transfer between them, but a polytropic process approximates the heat flow in the gas-liquid mixture. This process is in-between the extremes of isothermal and adiabatic processes. Cengel and Boles[18] emphasize that the fluid flow through a nozzle can be approximated as one dimensional isentropic flow (reversible adiabatic flow) with good accuracy.

In an adiabatic flow regime, there is no energy transfer with the surroundings. For a polytropic process, the pressure can be expressed as:

$$PV = RT = (C_p - C_v)dT \Rightarrow C_v dT = (C_v + C_p)\frac{T}{V}dV \quad \text{.....(1)}$$

Separating the variables, writing k representing C_p/C_v and integrating Eq. 1 yields

$$TV^{k-1} = \text{constant} \quad \text{.....(2)}$$

Eq. 2 implies temperature and volume relations for an ideal gas where an adiabatic expansion exists. Eliminating the temperature term and expressing Eq.2 on the basis of one unit of flowing gas yields:

$$Pv_g^k = \text{constant} \quad \text{.....(3)}$$

Cengel and Boles[18] emphasize that during expression and compression of real gases are often related by Eq. 3. Polytropic expansion occurs at downstream conditions.

The variables in Eq. 3 are the properties of gas inside the nozzle. However, the system has two phases, which include liquid and gas. The heat capacity of an incompressible liquid at constant pressure is equal to that at a constant volume. So, the heat capacity ratio of the fluid is:

$$k = n = \frac{(f_g C_{pg} + f_l C_{vl})}{(f_g C_{vg} + f_l C_{vl})} \quad \text{.....(4)}$$

To determine the sonic boundary, the magnitude of the discharge pressure in the restriction throat must be known. This is not normally measured directly. This can be expressed as P_2, as presented in Figure 1. On the other hand, pressure at the outlet of the nozzle throat, P_3, can be estimated by a pressure measurement device. For subsonic flow, Perkins[11] has developed an approximate relationship,

$$P_3 = P_1 - \frac{P_1 - P_4}{1 - (d_c/d_d)^{1.85}} \quad \text{.....(5)}$$

The General Energy Equation for Sonic and Sub-Sonic

The thermodynamic framework for multiphase sonic and sub-sonic flow is based on the principles of conservation of energy. For any point in the flowing system, the following assumptions are made:

1. Velocity varies with axial (flow) direction, but for a particular arbitrary point, all components are moving with the same velocity. According to Fortunati[9], when dealing with the two-phase flow, all the researchers found that both phases will have the same velocity, if velocity is greater than 10 m/sec and the Froude Number (Eq. 6) is greater than 600.

$$Fr = \left(\frac{\vartheta^2}{g_c d}\right) \quad \text{.....(6)}$$

2. Ros[2] showed that there is practically no slippage between the phases. Hence, it is reasonable to assume the same velocity for each phase at the nozzle.

3. The gas compressibility factor is depends on temperature and pressure. The liquid has a negligible compressibility when compared with gas.
4. Elevation changes are ignored.
5. The flow is adiabatic. (even the nozzle is not insulated). The process is so fast that the rate of heat transfer between the fluid flowing in the nozzle and the surroundings is zero.
6. The flow is frictionless. According to Ros[2], the wall shear forces can be ignored. Moreover, in mana's[1] experimental work, viscosity has a negligible effect on the pressure drop.
7. Temperature varies in the axial direction, but for an arbitrary point, all components are moving with the same temperature.

The general energy equation is evaluated by the method explained in Appendix A.

$$\left[\left(v_{f2}-v_l\right)\left(\frac{n}{n-1}\right)\left(P_2+\left(P_2^{\frac{n-1}{n}}P_1^{1/n}\right)\right)\right]+v_l\left(P_2-P_1\right) = \frac{\vartheta_1^2-\vartheta_2^2}{144\times 2g_c}-\left(\int_{T_1}^{T_2} C_{vf}\,dT\right) \quad \text{.....(7)}$$

In Eq. 7, the mass flow rate term is isentropic and at all cases, the isentropic value is equal to the ratio of the actual flow rate and the nozzle discharge coefficient. According to Perkins[11], after a compilation of 1,432 data sets from the literature, comprising both sonic and subsonic flows, the best overall average value of the discharge coefficient, C_N, is found to be 0.826.

The sound velocity for compressible fluid mixtures can be written as below. The deviation of the equation is explained in Appendix B.

$$\vartheta_s=\sqrt{n\frac{P_0}{\rho_0}} \quad \text{.....(8)}$$

Flow Diagram of the Model

1. The model requires the following inputs.
   - Bit inside and outside diameters are used in Eq. 5.
   - The number of nozzles and the nozzle size are used to calculated equivalent size of the nozzles.
   - Gas flow rate, in standard conditions, and liquid flow rate to estimate mass flow rates and mass fraction of the phases.
   - Bottom hole temperature and pressure.
   - The fluid inside the drill string gains heat from the surroundings. When the fluid reaches the bit, it is assumed that the temperature of the fluid is equal to the bottom hole temperature. Thus, the bottom hole temperature is referred as T_1.
2. If the bit has more than one nozzle, the model estimates an equivalent nozzle diameter, as given in Eq. 9.

$$d_{c-eq}=\sqrt{\sum_{i=1}^{NN} d_c^2} \quad \text{.....(9)}$$

3. As a first iteration, the value of downstream pressure, P_1 is equalized to P_4.
4. P_3 is calculated, by using Eq. 5 (Perry Relationship[14]). Subsonic velocity is used in this equation. The calculated pressure value is assumed to be equal to the nozzle pressure, i.e., P_2=P_3,
5. In order to determine the mass fraction, mass flow rates and the specific volume of liquid and gas phases, physical properties of the gas phase and the liquid phase and mixtures of these phases should be well defined. The proposed model requires gas compressibility. The compressibility factor of air can be calculated by using Papay's[20] method. Then, using the real gas equation ρ_{g1} and using volume fractions of the phase v_{f1} can be calculated.
6. The polytropic expansion exponent, n must be calculated. The model needs air and water heat capacity values. The specific heat capacity values for air are obtained from Cengel and Bole[18], and Hodgman[19]. The estimated values of air are used for correlating heat capacity at desired P and T. For water, Perkins[11] suggested 778 ft-lbf/lbm-°F or constant volume heat capacity.
7. T_2 at the nozzle must be calculated using Eq. 10. As mentioned earlier, a polytropic expansion occurs as the fluid accelerates downstream of the nozzle. For fluid flow, the temperature in the nozzle can be calculated as

$$\left(T_2+460\right)=\left(T_1+460\right)P_R^{(n-1)/n} \quad \text{.....(10)}$$

8. z_2, v_{f2} and ρ_{g2} should be calculated as mentioned in step 5.
9. The estimated mass flow rate must be calculated by using Eq. 11 and the conservation of mass rule is used for material balance.

$$\dot{m}_c=\dot{m}_a/C_N=\left(\left(q_l\times\rho_l\right)+\left(q_g\times\rho_g\right)\right)/C_N \quad \text{.....(11)}$$

10. The velocity of the fluid at any point at the bit could be calculated as shown in Eq. 12

$$\vartheta=\frac{m_c}{A}\left(\frac{f_g}{\rho_g}+\frac{f_l}{\rho_l}\right) \quad \text{.....(12)}$$

11. The average pressure and temperature values must be determined (average of T_1 and T_2 or average of P_1 and P_2). The polytropic expansion exponent, n, as mentioned in step 6 must be recalculated. In the final form of general energy equation, Eq. 7, polytropic expansion exponent is important. Although it varies with the temperature and the pressure of the fluid, the average value is used and it is estimated by using average temperature and pressure values.
12. The general energy equation, Eq. 7, must be used for

calculating P_1.

13. Go back to step 4 and iterate the P_1 values until the results converge. If the percent difference between the values of P_1 is less than 1.0×10^{-6}, the model gives the best P_1 values.
14. Check ϑ_2 value, whether the system is in subsonic flow range or not. If $\vartheta_{sonic}>\vartheta_2$ then the flow is subsonic.

$$\vartheta_{sonic} = \sqrt{n\frac{P_2}{\rho_{f2}}} \quad \text{.....(A.12)}$$

15. If the velocity is greater than sonic velocity, the program reduces the gas and liquid flow rates at the same proportion till the velocity goes below the sonic velocity.

Results and Discussions

In this study, a mathematical model for estimating the pressure drop at the bit for two-phase fluids is presented. While there are some similar applications in the published literature, the diversity of this proposed model is more sensitive to flow conditions and inner forces. The algorithm and related calculated process give more accurate results than the models previously developed. The proposed model could work in the subsonic – sonic flow conditions. Since sonic flow is not practical with drilling operations, the model obtains pressure drop results across the bit only in subsonic flow. If the flow is sonic, the proposed model suggests a change in liquid or gas flow rates, so that the flow is kept in subsonic flow ranges.

A computer program has been developed based on the proposed model. Using this program, runs were performed at a wide range of typical field conditions for various air-water mixture flow rates, using the discharge coefficient, C_N = 0.826. These values were used for comparison of the performance of the proposed model with the previously developed models. The conditions are listed in Table 1, where Case 1 is assigned as a base condition.

Flow Type Determination

As previously mentioned in theory, the proposed model initially assumes that, the flow pattern of two-phase fluids through the bit nozzles is a dispersed bubbly flow. In the literature, there are five distinct flow patterns for vertical upward flow, as shown on the two phase flow pattern map presented in Figure 2 (Kaya et. al.[17]). For this study, the calculated superficial velocities of the liquid and gas phases flowing through bit nozzle have been plotted on that map. It can be seen that, in all cases, the flow is in the dispersed flow regime.

As mentioned before, it is assumed that the velocity varies with axial (flow) direction, but at a particular arbitrary point, all components are moving with the same velocity (i.e. no radial gradients). Moreover, an assumption is made that no slippage occurs between the phases in the nozzle throat is. Two boundaries are specified to confirm these assumptions. For this study, the calculated velocity through the bit nozzle and Froude number were checked, as seen in Figure 3, and it is observed that calculated values are greater than these limits.

Comparison of Proposed Model With Previously Developed Models

Bit pressure drop predictions of the proposed model are compared with the existing ones, which are Gucuyener[14] and Liu[15] (Model I - Eq. (D-3)) and Guo[12] (Model II - Eq. (D-8)). This comparison was conducted in a range of practical values of bottom hole pressures and gas and liquid flow rates, as listed in Table 1. The comparison indicates that the differences between the models are very sensitive to changes in bottom hole pressure, gas and liquid flow rates.

Internal energy and temperature changes of flow of a two-phase fluid, which flows across a bit, are not included in the previous models. The proposed model does not ignore those changes for the bit pressure drop calculations. The existence of those factors affects the pressure drop values. The variations due to those factors are also examined.

Effect of Bottom Hole Pressure on Bit Pressure Drop

The comparison of the models was conducted for a constant liquid rate, varying bottom hole pressure, and gas flow rates. The results are plotted on graphs, as seen at Figure 4 and Figure 5. In these figures, the Proposed Model does not show a significant difference with Model I curves. However, significant differences are observed with the results of the Model II. The proposed model differs from Model I results by a maximum of 9%.

The effect of internal energy on bit pressure drop is not significant for lower bottom-hole pressures. Since, Model I does not include the internal energy and assumes that the velocity of the fluid at the bit, ϑ_1, is zero, the predicted results of the Proposed Model without internal energy effects shows a similar behavior. In the general energy equation, Eq. 7, the kinetic energy change depends on the inlet and outlet velocities of the fluid at the bit. Due to the Model I assumptions of zero inlet velocity of fluid, the kinetic energy values at upstream condition are zero and the calculated kinetic energy gain is higher for that model. This leads to a higher predicted bit pressure drop value. The existence of internal energy and factor of temperature changes in the bit result in a maximum 3.3% difference, Table 4.

The curves tend to come together with increasing bottom hole pressure, as seen in Figure 4. However, the predicted values of Model II are approaching to zero with an increase in bottom-hole pressure. The reason for this is that the existing gas is compressed and the volume of

the gas in the mixture is reduced, i.e., the gas concentration reduces. Actually, Model II is valid for high gas concentrations.

For drilling operations, sonic flow is not practical. As shown in Figure 5, the proposed model indicates there is a sonic boundary for higher gas flow rates.

Effect of Liquid Flow Rate on Bit Pressure Drop

The effects of bit pressure drop with varying liquid rates at two different bottom hole pressure values on bit pressure drop are examined, Figure 6. At 750 and 1750 psi bottom hole pressures, the curves are approaching to each other except for the curve of Model II. The results of Model I and the proposed model are close to each other. But, although the quantity is small, the variation increases with an increase in liquid flow rate.

The internal energy term effect on the bit pressure drop is not significant, Figure 6. As the bottom hole pressure increases, the effect is more significant. In fact, the heat capacity constant, which is a variable of internal energy term, is depend on pressure. Therefore, as the bottom hole pressure is increases, the internal energy term on general energy equation would be more dominant.

Conclusions

In this study, a mathematical model has been developed for calculating the pressure drop across a bit nozzle for two phase drilling fluids. The general energy equation and the sound wave transmission concept are used as the basis of the proposed model. This model is valid for both sonic and subsonic flow. Data for air–water mixtures have been used for testing the performance of the proposed model. The conclusions obtained are listed below:

1. In this study, it has been shown that the flow pattern is the dispersed bubbly flow through the bit nozzles. Moreover, the assumptions that both phases are moving with the same velocity at any arbitrary point, and that there is no slippage between the phases at the nozzle throat, are substantiated.
2. Since sonic flow through the nozzle is not desired in drilling operations, the model calculates the pressure drop at the bit for subsonic conditions. If the flow is sonic, the model changes the liquid and gas flow rates to achieve subsonic conditions.
3. The proposed model can calculate the pressure drop across the bit with reasonable accuracy. It shows a maximum 9% difference with the Model I results.
4. The strength of the proposed model, relative to other models, is that it takes into account the effects of internal energy and temperature changes. These features improve the accuracy of the pressure drop calculations across the bit.
5. The most widely used model in the drilling industry, Model I under-estimates the pressure drop at the bit, while Model II overestimates the pressure drop across the bit.
   - Model II is valid only for high gas flow rates and high gas fractions. Model II predicts lower pressure drops than Model I, and the proposed model.
   - The internal energy, compressibility factor, temperature changes, and initial kinetic energy term do not have any effect on Model II results, because the effects of those factors are not included in those models. Indeed, the elimination of initial kinetic energy term in Model II is the major factor of the variation with the proposed model.
   - When the internal energy term is ignored, the proposed model gives closer results to Model I. The internal energy changes in the proposed model reduce the bit pressure drop values about 3.3%, relative to the other models considered in this study.

Acknowledgments

The authors wish to express their appreciation to Turkish Petroleum Co., for supporting this project, and for allowing publication of this study.

Nomenclature

A	= Area, ft
C_p	= Isobaric heat capacity, (ft-lbf)/(lbm-°F)
C_v	= Isotropic heat capacity, (ft-lbf)/(lbm-°F)
C_N	= Nozzle discharge coefficient, dimensionless
d_c	= Nozzle diameter, ft
$d_{c\text{-}eq}$	= Equivalent diameter of nozzles, ft
d_d	= Pipe diameter downstream of the nozzle, ft
E	= Internal energy of one pound fluid, ft-lbf/lbm
f	= Weight fraction in the flowing fluid, dimensionless
F	= Heat capacity ratio, dimensionless
g	= Acceleration of gravity, ft/sec^2
g_c	= 32.2 (lbm-ft)/(lbf-sec^2)
k	= Heat capacity ratio
k_e	= Kinetic energy of one pound fluid, (ft-lbf)/lbm
m	= Mass, lbm
$\dot{m}_c$	= Calculated mass flow rate, lbm/sec
$\dot{m}_a$	= Actual mass flow rate, lbm/sec
NN	= Number of nozzles, dimensionless
n	= Polytropic expansion exponent, dimensionless
P	= Pressure, psi
P_B	= Bit Pressure Drop across the bit , psi
P_R	= Pressure drop ratio, dimensionless
pe	= Potential energy of one pound fluid, (ft-lbf)/lbm
PE	= Potential energy, ft-lbf
Q	= Heat transferred to one pound of the flowing fluid, (ft-lbm)/lbm
q	= Flow rate, cuft/sec

q_{gsc} = *Flow rate at standard conditions, scft/sec*
R = *Universal gas constant (psi-ft^3)/(lbm-mol-$^\circ$R)*
T = *Temperature, $^\circ$F*
W = *Work, ft-lbf*
w = *Work of one pound fluid, (ft-lbf)/lbm*
V = *Volume, cuft*
z = *Gas compressibility factor, dimensionless*
Z = *Elevation, ft*

Greek Letters
ϑ = *Velocity, ft/sec*
κ = *Elasticity, psi*
β = *Volumetric fraction, dimensionless*
ν = *Specific volume, ft^3/lbm*
ρ = *Density, lbm/ft^3*

Subscripts
f = *fluid*
g = *gas*
l = *liquid*
m = *mixture*
BH = *bottom hole*
0 = *initial*
1 = *upstream of the nozzle*
2 = *at the nozzle throat*
3 = *condition just downstream of the nozzle throat if flow is subsonic*
4 = *recovered condition downstream of polytropic compression.*

References

1. Omana, R. et. al.: “Multiphase Flow Through chokes,” paper SPE 2682 presented at the 1969 SPE Annual Meeting, Denver, Sept. 28-Oct. 1.
2. Ros, N.C.J.: “An Analysis of Critical Simultaneous Gas-Liquid Flow Through a Restriction and its-Application To Flow Metering,” Applied Sci. Research (1960), 2, Section A, 374.
3. Pilehvari, A.A.: “Experimental Study of Critical Two-Phase Flow Through Wellhead Chokes” U. of Tulsa Fluid Flow Project, June 1981
4. Osman, M.E. and Dokla, M.E.: “Gas Condensate Flow Through Chokes,” SPE Paper 20988, 23 April 1990.
5. Tangren, R. F., Dodge, C. H., and Seifert, H.S.: “Compressibility Effects in Two-Phase Flow,” J. Appl, Phys. (July 1949) 20,637.
6. Ashford, F. E.: “An Evaluation of Critical Multiphase Flow Performance Through Wellhead Chokes,” JPT (Aug. 1974) 843.
7. Ashford, F. E. and Fierce, P. E.: “Determining Multiphase Pressure Drop and Flow Capabilities in Down-Hole Safety valves,”, JPT (Sept.1975) 1145.
8. Sachdeva, R., Schmidt, Z., Brill, J.P. and Blais, R.M.: “Two-Phase Flow Through Chokes,” paper SPE 15657 presented at the 1986 SPE Annual Technical Conference and Exhibition, New Orleans, Oct. 5–8.
9. Fortunati, F.: “Two-Phase Flow Through Wellhead Chokes,” paper SPE 3742 presented at the 1972 SPE European Spring Meeting, The Netherlands, May 16-18.
10. Gould, T. L.: ‘Discussion of an Evaluation of Critical Multiphase Flow Performance Through Wellhead chokes,” JPT (Aug. 1974) 849.
11. Perkins, T.K.: ”Critical and Subcritical Flow of Multiphase Mixtures Through Chokes” SPE Drilling & Completion, December 1993.
12. Guo, B., Harelend, G., Rajtar, J.: “Computer Simulation Predicts Unfavorable Mud Rate and Optimum Air Injection Rate for Aerated Mud Drilling” paper SPE 26892 presented at the 1993 regional Conference & Exhibition held in Pittsburgh, PA, Nov. 2–4.
13. Lynos, W.C., Guo, B. and Seidel, F.A., Air and Gas Drilling Manual, McGraw-Hill, New York (1999).
14. Gucuyener, İ. H.: “Design of Aerated Mud for Low Pressure Drilling” paper SPE 80491 presented at the 2003 SPE Asia Pacific Oil and Gas Conference and Exhibition held in Jakarta, Indonesia, April 15–17.
15. Liu, G. and Medley, G.H.: “Foam Computer Model Helps in Analysis of Under balanced Drilling” Oil and Gas J. July 1, 1996, p.114-119
16. Wood, A. B., A Testbook of Sound, G. Bell and Sons LTD, London (1960).
17. Kaya, A.S., Sarica, C., Brill, J.P. : “Comprehensive Mechanistic Modeling of Two-Phase Flow in Deviated Wells,” paper SPE 56522 prepared for presentation at the 1999 SPE Annual Technical Conference and Exhibition held in Houston, Texas, 3–6 Oct. 1999.
18. Cengel, Y.A., Boles, M.A., Thermodynamics: An Engineering Approach, 2nd edition, McGraw-Hill Book Co., Inc., New York City, (1994) 870
19. Hodgman, C.D., Holmes, H.N., Handbook of Chemistry and Physics, 25th edition, Chemical Rubber Publishing Co., Cleveland, Ohio, (1941).
20. Papay, J.: “A Termelestechnologiai Parameterek Voltozaa a Gazle-lepk Muveless Soran,” OGIL MUSZ, Tnd, Kuzl., Budapest (1968) 267.

Appendix A – Derivation of The General Energy Equation

A fundamental law of nature is the principle of the conservation of energy. The first law of thermodynamics is simply an expression of the conservation of energy principle.

$$dw_{flow} + dE + dke + dpe + dQ + dW = 0 \quad \text{..... (A-1)}$$

The mathematical modeling of two–phase flow can be developed on the bases of the general energy equation. In the flow direction, there are four important points, as seen in Figure 1. At point 1, the velocity is low, compared to the velocity at point 2. In addition at point 1, although the pressure is an unknown at this moment, the kinetic and internal energies can be used to determine P_1. The fluid passes to point 2, i.e. flows through the nozzles. Since the fluid accelerates, there is a kinetic energy increase through the nozzle, in other words, energy changes form from flow work to kinetic energy. Then, the fluid is decompressed and a polytropic expansion occurs. Because there is no heat transfer, at point 2, the temperature reduces due to the sudden adiabatic expansion. Unfortunately, pressure cannot be

measured at point 2. However, the pressure at the outlet of the nozzle throat, P_3, can be determined by a pressure measurement device. For subsonic flow, P_3 equals P_2, when the fluid reaches point 4, it has reached the final state of energy, pressure, and temperature values. Since a portion of kinetic energy is lost at the discharge of the nozzle due to the polytropic expansion, the pressure difference between points 4 and 3 is small. The relation between P_3 and P_4 is expressed by Eq. 5.

The energy changes of the fluid are explained, before the fluid pass from point 1 to point 2. On the basis of one pound of flowing fluid, the general energy equation can be written as:

$$144\left(Pd\nu+\nu dP\right)+d\left(C_{vf}T\right)+\frac{1}{2g_c}2\vartheta d\vartheta+\frac{g}{g_c}dZ+dQ-dW=0 \quad \text{.....(A-2)}$$

Initially, because of the small size of the nozzle, the difference in elevation is negligible. Since, there is neither work done on the system nor work done by the system, overall work equals zero. Moreover the heat transfer is also assumed to be negligible, W = 0 and $Q\cong 0$.

Thus, the general energy, Eq. A-2 equation reduces to Eq. A.-3.

$$144\left(Pd\nu+\nu dP\right)+d\left(C_{vf}T\right)+\frac{1}{2g_c}2\vartheta d\vartheta=0 \quad \text{.....(A-3)}$$

For a given control volume, integration of Eq. A-3 yields

$$144\int_{P_1}^{P_2}\nu dP+\int_{T_1}^{T_2}C_{vf}dT+\frac{1}{g_c}\int_{\vartheta_1}^{\vartheta_2}\vartheta d\vartheta=0 \quad \text{.....(A-4)}$$

As mentioned above, the polytropic expansion occurs as the fluid accelerates through the nozzle. The polytropic expansion equation, in terms of the specific volume of gas, between points 1 and 2, for a confining pressure, P, polytropic expansion constant, b, and ratio of specific heat constant n, is given below.

$$P_1\left(\nu_{f1}-\nu_l\right)^n=P_2\left(\nu_{f2}-\nu_l\right)^n \quad \text{.....(A-5)}$$

So, the first term of Eq. A-4 becomes

$$144b^{1/n}\left(\frac{n}{n-1}\right)\left(P_2^{\frac{n-1}{n}}-P_1^{\frac{n-1}{n}}\right)+144\nu_l\left(P_2-P_1\right) \quad \text{.....(A-6)}$$

Integrating Eq. A-6 into Eq. A-4 yields

$$144b^{1/n}\left(\frac{n}{n-1}\right)\left(P_2^{\frac{n-1}{n}}-P_1^{\frac{n-1}{n}}\right)+144\nu_l\left(P_2-P_1\right)+\left(\int_{T_1}^{T_2}C_{vf}dT\right)+\frac{\vartheta_2^2-\vartheta_1^2}{2g_c}=0 \quad \text{.....(A-7)}$$

Combining Eq. A-6 and Eq. A-7 give the final form of general energy equation

$$144\left\{\begin{bmatrix}\left(\nu_{f2}-\nu_l\right)\left(\frac{n}{n-1}\right)\left(P_2+\left(P_2^{\frac{n-1}{n}}P_1^{1/n}\right)\right)\end{bmatrix}+\nu_l\left(P_2-P_1\right)\right\}=\frac{\vartheta_1^2-\vartheta_2^2}{2g_c}-\left(\int_{T_1}^{T_2}C_{vf}dT\right) \quad \text{.....(A-8)}$$

Appendix B – Velocity of Wave Transmission

The sound velocity is influenced by the physical properties of the medium, such as density and elasticity, which are equivalent to the mass as a stiffness factor in the case of vibration of a particle, as stated by Wood[16]. While a wave of compression and rarefaction moves through a medium, the density (i.e. the volume) fluctuates locally. The value of these fluctuations depends on the fluid properties as well as the applied force (power of sound). To clarify the behavior of the sound wave, the dilation, condensation, elasticity, and density of the medium are examined. Wood[16] has developed an approximate relationship for all cases of transmission of a small amplitude plane wave in solid, liquid or gaseous media.

$$\vartheta_s=\sqrt{\frac{\kappa}{\rho_0}} \quad \text{.....(B-1)}$$

In the gas-liquid medium, it can be assumed that ρP_0=constant for a constant temperature. So, the elasticity is reduced to,

$$\kappa=-V_0\frac{\partial P}{\partial V}\Rightarrow\kappa=P_0 \quad \text{.....(B-3)}$$

If the system is not isothermal, but adiabatic, using Eq. 3 and Eq. B-2, the equality becomes

$$P\nu^n=P_0\nu_0^n\Rightarrow\kappa=nP_0 \quad \text{.....(B-4)}$$

Combining Eq. B-1 and Eq. B-3, the sound velocity for compressible fluid mixtures can be written as

$$\vartheta_s=\sqrt{n\frac{P_0}{\rho_0}} \quad \text{.....(B-5)}$$

Appendix C – Correlation Of Air Properties

Correlation for Air Heat Capacity at Constant Pressure

The developed computer program based on the proposed model also calculates the heat capacity values measured by Cengel and Bole[18], and Hodgman[19] values, Table 2. The measured values are numerically processed by the computer and the results are obtained at given pressures and temperatures.

Gas Compressibility Factor For Air

The air compressibility factor, *z*, is estimated using Papay's[20] method, which is given by.

$$z = 1.0 - \left(\frac{P_r}{T_r}\right)\left[0.36748758 - 0.04188423\left(\frac{P_r}{T_r}\right)\right] \quad \text{.....(C-1)}$$

In this equation, the reduced pressure, P_r , and the reduced temperature, T_r , of air are given by,

$$P_r = P/547 \quad \text{.....(C-2)}$$

$$T_r = (T + 460)/239 \quad \text{.....(C-3)}$$

Appendix D – Existing Models

Model I - Gucuyener and Liu Model

Gucuyener[14] and Liu[15] developed an equation for determination of pressure drop across the nozzle. In their studies, the general energy equation for two-phase flow through the bit nozzles was used for developing the bit pressure drop equation.

$$v_f dP + \frac{1}{g_c}\vartheta_f d\vartheta_f + dE + \frac{g}{g_c}dZ = 0 \quad \text{.....(D-1)}$$

It was assumed that the volumetric velocity of the fluid is almost zero at the upstream conditions. Therefore, the upstream velocity of the fluid was assigned to zero. Moreover, the elevation changes and internal energy term in the general energy equation were neglected because of their slight effect on the calculations. Thus, the integration of Eq. (D-1) becomes,

$$\int_{P_{up}}^{P_{BH}} v_f dP + \frac{1}{g_c}\int_0^{\vartheta_{nozzle}} \vartheta_f d\vartheta_f = 0 \quad \text{.....(D-2)}$$

$$\left\{\begin{array}{l} 1.08\times10^{-4}\left(\dfrac{\vartheta_{nozzle}}{C_N}\right)^2 - \dfrac{f_l}{\rho_l}(P_B) \\ + \dfrac{f_g}{\rho_g} P_{BH}\left(\ln\dfrac{P_{BH}}{P_{BH}-P_B}\right) \end{array}\right\} = 0 \quad \text{.....(D-3)}$$

The results of the equation were compared with those of the proposed model. The results of the Gucuyener[14] and Liu[15] equation overestimate the pressure drop of the bit.

Model II - Guo Model

Guo, et. al.[12] developed an equation for estimating the pressure drop of a multiphase fluid flow through a nozzle. From the first law of thermodynamics, the following equation was obtained.

$$\frac{dP}{\rho_f} + \frac{\vartheta_f}{g_c}d\vartheta_f + \frac{g}{g_c}dZ = 0 \quad \text{.....(D-4)}$$

According to their study, the elevation changes and energy losses caused by friction were neglected. So, Eq. (D-4) became

$$dP = -\frac{\rho_f}{g_c}\vartheta_f d\vartheta_f \quad \text{.....(D-5)}$$

$$P_{upstream} - P_{downstream} = \frac{\rho_m}{2g_c}\left(\vartheta^2_{f-down} - \vartheta^2_{f-up}\right) \quad \text{.....(D-6)}$$

The velocity of a fluid can be determined as

$$\vartheta_f = \frac{\dot{m}_f}{\rho_f \times A_{nozzle}} \quad \text{.....(D-7)}$$

Thus, substituting Eq. (D-6) into Eq. (D-7) yields

$$P_B = \left(\frac{\dot{m}_f}{A_{nozzle}}\right)^2 \frac{1}{g_c \times 144}\left(v_{f-down} - v_{f-up}\right) \quad \text{.....(D-8)}$$

Equation (D-8) depends on the specific volume of the fluid. For incompressible mixtures or fluids, the specific volume difference in the equation reduced to zero. Therefore, the equation is valid only for compressible fluids.

Appendix E – Variation and Iteration Error Analyses

Iteration Analysis

The developed computer program does calculation processes containing iterations. After iterations, the program calculates the difference between the consecutive iterated values and compares the difference with desired error. The desired iteration error value is defined by the user, and assigned to get more accurate results. The iteration error values and obtained result values are listed in Table 3. For calculation of the pressure drop values, the error value of 1.0×10^{-6} is selected for iteration error.

Variation Analysis

The following statistical parameters have been used to compute the accuracy of the investigated correlation.
Average absolute percent relative deviation:

$$APD = (1/k)\sum_{i=1}^{k} PD_i \quad \text{.....(E-1)}$$

$$PD_i = \left(\left(P_{Bo} - P_{Bm}\right)/P_{Bo}\right)\times 100 \quad \text{.....(E-2)}$$

where
k= 1, 2, 3, 4,….
P_{Bm} is bit pressure calculated by the proposed model
P_{Bo} is bit pressure calculated by the existing model

Standard deviation:

$$SD = \sqrt{\frac{k\left(\left(\sum_{i=1}^{k} PD_i^2\right) - \left(\sum_{i=1}^{k} PD_i\right)^2\right)}{k(k-1)}} \quad \text{.....(E-3)}$$

Table 1. Selected Parameters For Sample Run

	Case 1	**Case 2**	**Case 3**	**Case 4**
Gas Phase	Air	Air	Air	Air
Liquid Phase	Water	Water	Water	Water
Number of Nozzles	3	3	3	3
Nozzle Size, in	13/32	13/32	15/32	13/32
Diameter of downstream, in	12 ¼	12 ¼	12 ¼	8 ½
Diameter of upstream, in	2 ¼	2 ¼	2 ¼	1 ¾
Q_{GSC}, scft/min.	200 500 750 1000 1500	200 500 750 1000 1500	200 500 750 1000 1500	200 500 750 1000 1500
Q_{liq}, gal/min	100 200 300	100 200 300	100 200 300	100 200 300
P_{BH}, psi	250 500 750 1250 1750	250 500 750 1250 1750	250 500 750 1250 1750	250 500 750 1250 1750
T_{BH}, °F	100	150	100	100

Table 2 Constant Pressure Heat Capacity Values

	Temperature, °F			
Pressure, psi	-58	32	122	212
14.7	186.7139	186.5582	186.8687	187.5387
147	190.3492	189.6079	189.5775	190.2572
294	196.1764	194.3088	192.9859	192.2077
588	213.2961	202.7014	197.0065	196.2121
1029	242.8665	218.6682	204.4515	200.2164
1470	301.3886	250.2086	211.5842	202.3239
3234		714.9144	230.4158	221.0778
				C_p, ft-lbf/lbm-°F

Table 3 Iteration Error Analysis

Error	1.0×10^{-4}	1.0×10^{-5}	1.0×10^{-6}	1.0×10^{-7}
Calculated P_B	1209.0864745	1241.6502137	1245.0172463	1245.3350807

Table 4 P_B values of Case 1 at q_l=100 gal/min and P_{BH}=1750psi

q_{gsc}	**Model without Internal Energy**		**Model I**		**Model II**	
scft/min	**PD**	**|PD|**	**PD**	**|PD|**	**PD**	**|PD|**
0	0.000	0.000	1.486	1.486		
200	1.964	1.964	5.668	5.668	-9885.714	9885.714
500	3.894	3.894	9.681	9.681	-3725.000	3725.000
750	4.702	4.702	11.502	11.502	-2418.182	2418.182
1000	4.921	4.921	12.271	12.271	-1716.000	1716.000
1500	4.493	4.493	12.369	12.369	-1091.209	1091.209
Average	3.329	3.329	8.829	8.829	-3767.221	3767.221
SD	1.952	1.952	4.385	4.385	3557.604	3557.604

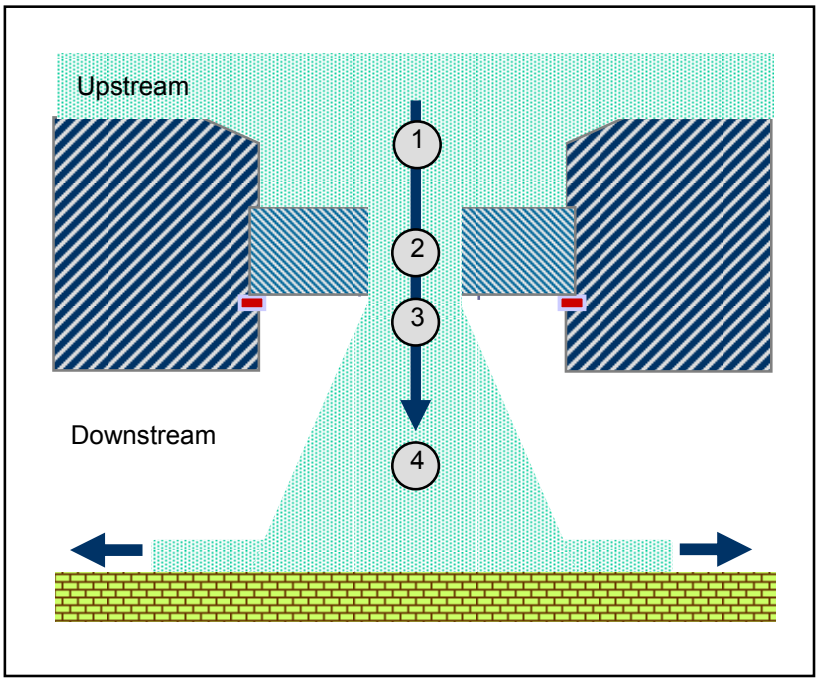

Figure 1. Diagram of Flow Through A Nozzle

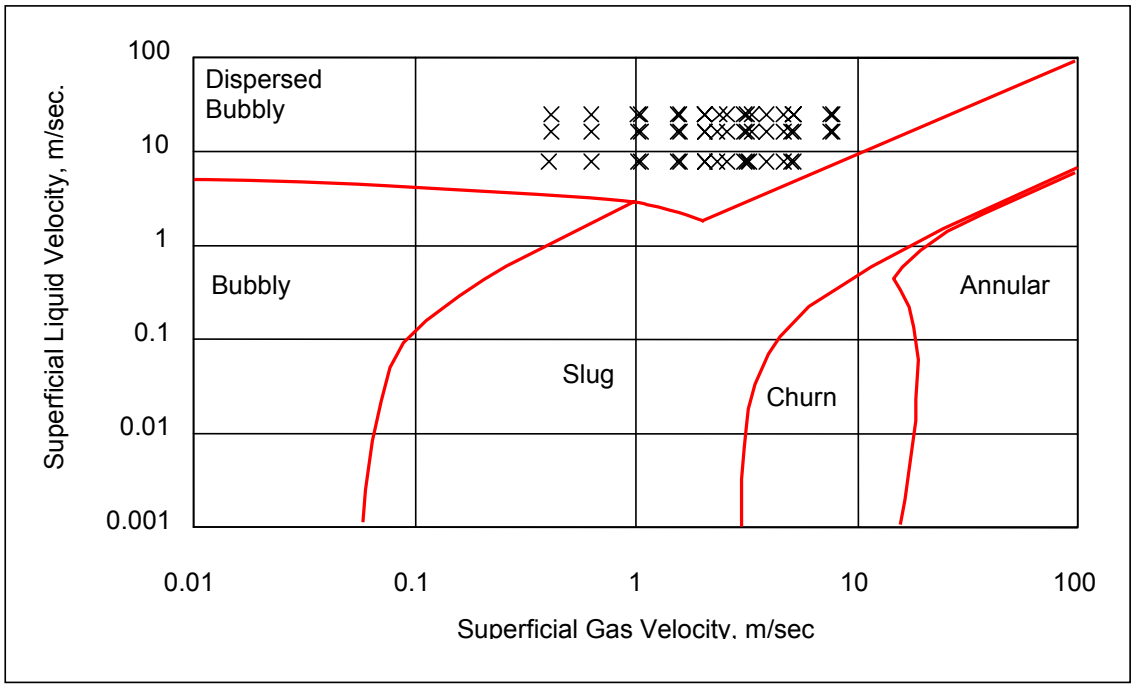

Figure 2. Two Phase Flow Map For Vertical Flow

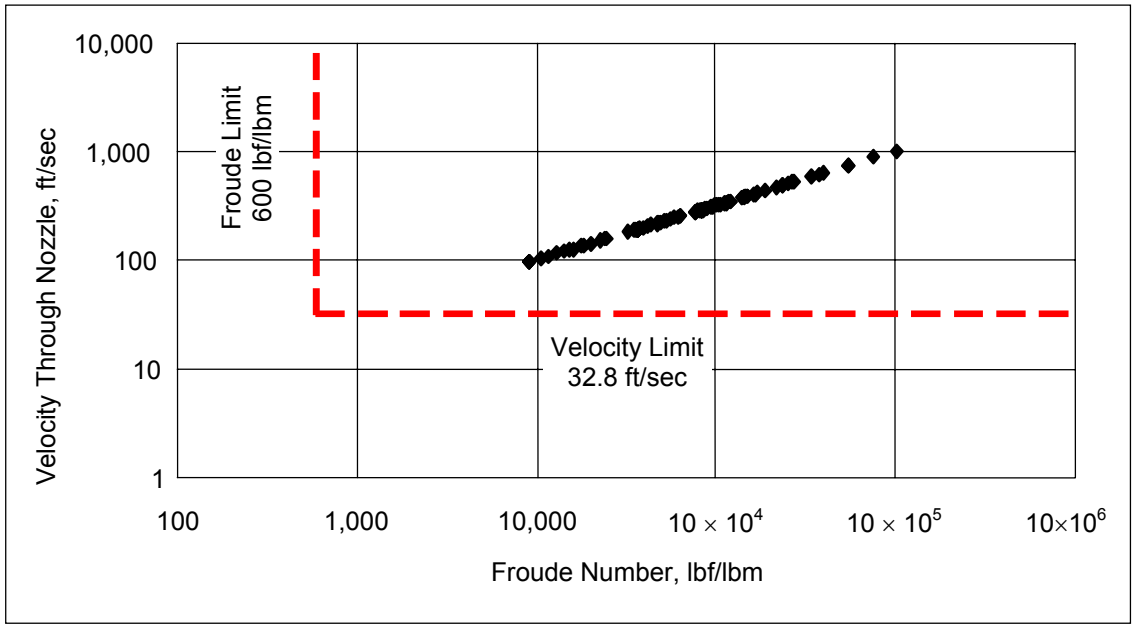

Figure 3. Froude Number and Fluid Velocity Through Nozzle

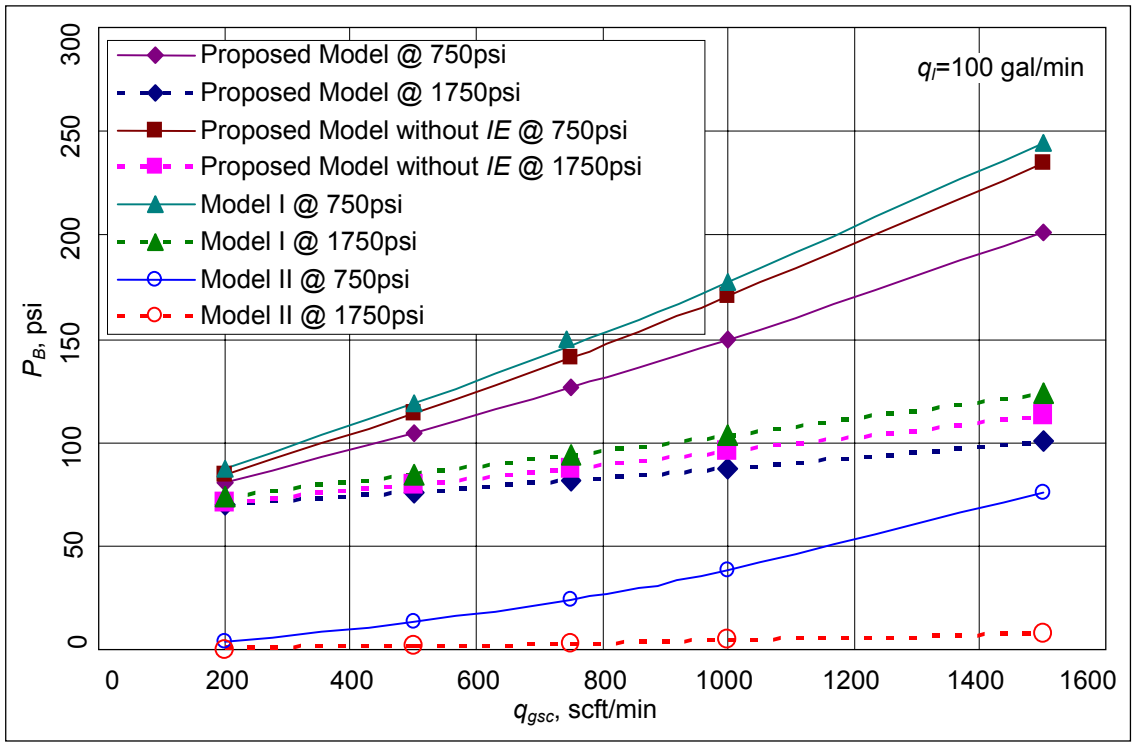

Figure 4. Comparison of The Models at Different Bottom Hole Pressures

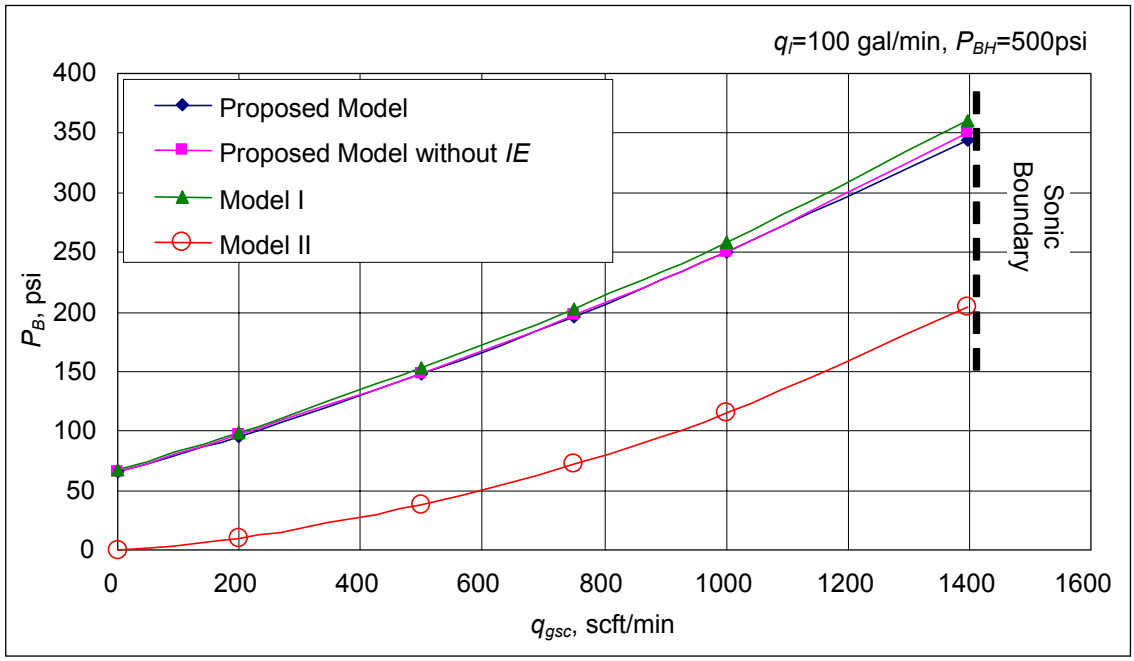

Figure 5. Comparison of The Models at Constant Bottom Hole Pressure and Liquid Flow Rate

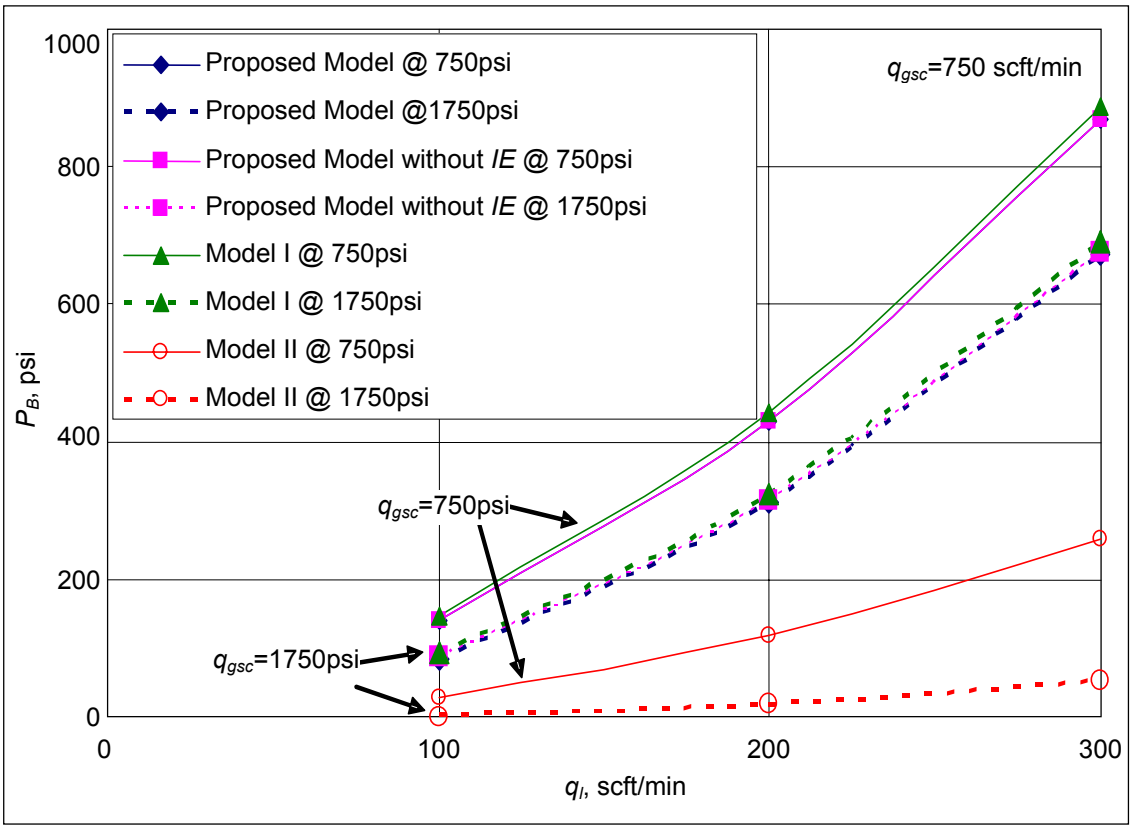

Figure 6. Comparison of The Models at Constant Gas Flow Rate